MIT Open Access Articles

Switching and Counting With Atomic Vapors in Photonic-Crystal Fibers

Massachusetts Institute of Technology

Switching and counting with atomic vapors in photonic-crystal fibers

Thibault Peyronel[†], Michal Bajcsy[†], Sebastian Hofferberth[†],
Vlatko Balic, Mohammad Hafezi, Qiyu Liang, Alexander Zibrov, Vladan Vuletic, and Mikhail D. Lukin

Abstract—We review our recent experiments demonstrating a hollow-core photonic-crystal fiber loaded with laser-cooled atomic vapor as a system for all-optical switching with pulses containing few hundred photons. Additionally, we discuss the outlooks for improving the efficiency of this switching scheme and present preliminary results geared toward using the system as a photon-number resolving detector.

Index Terms—All-optical switching, electromagnetically-induced transparency, laser-cooled atoms in hollow-waveguides, photon number detection.

I. Introduction

THE implementation of few-photon nonlinear optics has until now only been feasible in the context of cavity quantum electrodynamics (QED) when single quantum emitters, such as neutral atoms or quantum dots, are placed inside narrow-band, high-finesse cavities. In these systems, the original nonlinearities of the optical medium created by the single emitter are amplified by the cavity finesse to the point where they can be controlled by the field of a single photon. Over the last decade, several experiments have demonstrated nonlinear optical phenomena with single intracavity photons [1], [2], [3], [4]. However, the large nonlinearities achievable in these cavity-based systems come at the price of technological complexity, limitations imposed by cavity bandwidth, and often times substantial losses at the input and output of the cavity. The work presented here uses an alternative approach, which is based on coupling single emitters or ensembles of emitters to a propagating light field confined to an area comparable to the diffraction limit. This results in the electric field from a single photon being sufficiently large to cause nonlinear behavior on a single pass and without the environment of an optical cavity. Such tight confinement can be achieved either in free space by focusing the light beam with a large numerical aperture lens [5] or under conditions provided by a photonic waveguide. In particular, systems based on hollow core photonic crystal fibers [6], hollow antiresonant reflecting waveguides (ARROWs) [7], optical nanofibers [8], and nanostructure plasmonic waveguides allowing subdiffraction propagation [9] have all been actively explored in the last few years. Hollow core photonic crystal fibers (PCFs, also known as photonic bandgap fibers), that guide light through interference [10] instead of total internal reflection [11], are now available off the shelf and can be integrated with conventional optical fibers [12]. When
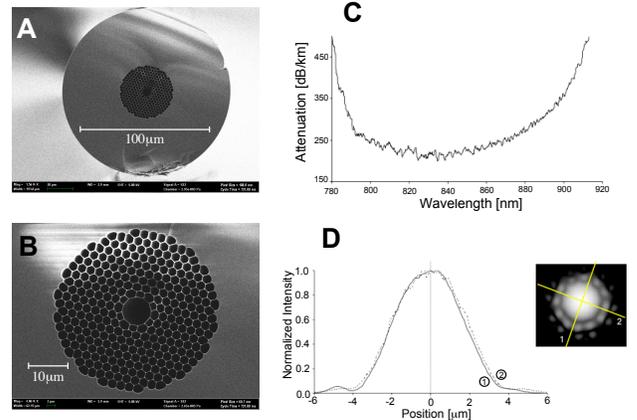
Fig. 1. (A) Scanning electron microscope (SEM) image of a cross section of the hollow-core photonic-crystal fiber from Blaze Photonics used in the experiment (model *HC-800-02*). (B) Detail of the photonic crystal region of the fiber with the hollow core in the center. Manufacturer's specifications of (C) losses of guided mode propagating in the fiber as a function of wavelength and (D) near field intensity distribution of the guided mode.

filled with molecular gas, these fibers have shown significant enhancements in the efficiency of processes such as stimulated Raman scattering [13] and four-wave mixing [14]. Recently, both room-temperature and ultra-cold atoms have successfully been loaded into PCFs [15], [16], [17] and observations of electromagnetically induced transparency with less than a micro-Watt control field have been reported for the case of room temperature atoms [15].

Here, we review our experiments that demonstrate the strong coupling between light and laser-cooled atoms inside the hollow core PCF and allow us to implement all-optical switching controlled with light pulses containing as few as several hundred photons.

II. Atoms inside the fiber

The atoms are first laser-cooled and collected in a free-space magneto-optical trap and then transferred into a 30mm long piece of hollow-core fiber (Fig. 1) with a procedure described in detail in Ref. [18]. Once inside the fiber core, the cold atoms are confined in a red detuned dipole trap [19]. The trap is created with an off-resonant beam guided by the fiber, and it prevents the atoms from colliding with the fiber wall. We probe the atoms, which form an approximately 1cm long cloud inside the fiber core [18], by monitoring the transmission of very-low-power ($\sim 1\,\mathrm{pW}$) probe beams that can be coupled into the fiber piece from either of its ends. After

the probe beams emerge from the fiber, they are collimated by the coupling lenses and then passed through a series of optical filters that separate the probe photons from other light beams coupled into the fiber during the experiments. Finally, the probes are coupled into single-mode fibers connected to single-photon counters. The use of single-mode fibers provides spatial filtering that ensures that only photons propagating in the guided mode of the PCF are detected. When the frequency of the probe laser is scanned over an atomic resonance, we observe in the transmitted signal an approximately Lorentzian absorption line-shape from the atoms present inside the fiber:

$$T_{nat} = \exp\left(-\frac{OD}{1+4(\frac{\delta_p}{\Gamma_e})^2}\right), \tag{1}$$

where Γ_e is the linewidth of the excited atomic state and $\delta_p = \omega_p - \omega_0$ is the detuning of the probe laser from resonance. The optical depth OD is a figure of merit for the strength of the observed absorption. In general, OD depends on the atomic density integrated along the fiber, and the strength of the considered atomic transition. Since the atoms are confined within the optical trap created by the guided light inside the fiber, the radial extent of the atomic cloud is smaller than the beam area of the single-mode probe light beam propagating through the fiber. To get an accurate relation between optical depth and atomic density inside the fiber, we have to take into account the atoms' radial distribution in the probe beam. In particular, an atom at the edge of a beam experiences a smaller electric field and therefore absorbs less light than an atom on the beam's axis. Assuming a Gaussian beam with waist w_o and a radially symmetric atomic density $n(r,z)$, the expression for optical depth on resonance is

$$OD_{fiber} = \frac{2}{\pi w_o^2} \int_{L_{cloud}} 2\pi \int_0^{r_{core}} n(z,r)c_{CG}^2\sigma_o e^{-\frac{2r^2}{w_o^2}} rdrdz \tag{2}$$

where $\sigma_o = \frac{3\lambda^2}{2\pi}$ is the maximal atomic cross-section, and c_{CG} is the Clebsch-Gordon coefficient for the specific atomic transition being used. In general, (2) reduces to a simple expression that shows that OD is proportional to the number of atoms N_{at} inside the fiber:

$$OD_{fiber} = \eta N_{at} \frac{2c_{CG}^2\sigma_o}{\pi w_0^2}. \tag{3}$$

The prefactor η is given by the radial distribution of atoms in the fiber-confined cloud. The highest value of η corresponds to all atoms being localized on the axis of the fiber, in which case $\eta = 2$. In the case of a Gaussian radial density distribution $n(r) = n_0 e^{-\frac{r^2}{2x_0^2}}$, $\eta = \frac{2(w_0/2)^2}{x_0^2+(w_0/2)^2}$. The optical depth of the atomic cloud inside the fiber is thus determined by the number and temperature of atoms inside the fiber. In particular, higher atomic temperatures lead to more axially delocalized cloud (increased x_0), which in turn results in decreased OD. Assuming an atomic temperature $T \sim 1\,mK$ and using the measured beam waist of guided light inside the fiber $w_0 = 1.9 \pm 0.2\,\mu m$, ~ 100 atoms inside the fiber create an optically dense medium ($OD = 1$) when probed at the transition with the highest Clebsch-Gordon coefficient.
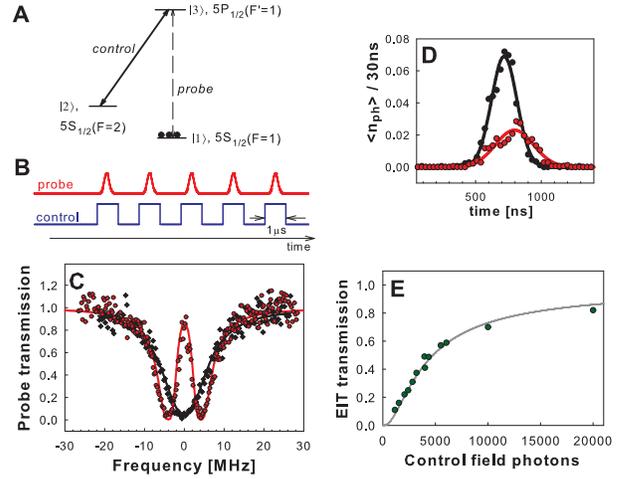

Fig. 2. (color online) (A) The atomic level scheme and the corresponding hyperfine states of rubidium^{87} used in the EIT demonstration. (B) Both probe and control field are broken into a set of ~ 100 synchronized pulses sent through the fiber during the off-times of the dipole trap. (C) Transmission of the probe light through the fiber as a function of detuning from resonance in the presence of the control field (red data). The black data show probe transmission without the control field. (D) Individual probe pulse shape and delay. Here, $\langle n_{ph} \rangle$ represents the average number of photons detected in a 30 ns time bin. The reference pulse (black) is obtained without the presence of atoms inside the fiber. The red pulse is delayed due to the group velocity reduction in the atomic medium under EIT conditions. (E) Observed transmission of the probe pulses on resonance as a function of average number of photons in the $1\,\mu s$ control field pulse and the prediction (grey line) obtained by evaluating equation (2) in Ref. [24].

III. ALL-OPTICAL SWITCHING

The mechanism used here for all-optical switching is based on electromagnetically induced transparency (EIT) [20], [21]. In this phenomenon, an atomic ensemble, which is originally opaque for a resonant probe beam, is changed to transparent with the help of a control beam. For this we consider the 3-state Λ-configuration of atomic states shown in Fig. 2A. In the presence of a strong control field, the weak probe field, resonant with the $|1\rangle \rightarrow |3\rangle$ transition, is transmitted without loss. The essence of EIT is the creation of a coupled excitation of probe photons and atomic spins ("dark-state polariton") [22] that propagates through the atomic medium with greatly reduced group velocity [23] and can be efficiently manipulated.

To demonstrate EIT, we first prepare the atoms in the $F = 1$ ground state, and then probe the medium with a linearly polarized probe tuned to the D1 $F = 1 \rightarrow F' = 1$ transition. In the absence of the control beam, the medium is completely opaque at resonance (Fig. 2C, black data points). In contrast, when a co-propagating control field resonant with the $F = 2 \rightarrow F' = 1$ transition is added, the atomic ensemble becomes transparent near the probe resonance (Fig. 2C, red data points). Figure 2D shows the individual pulse shape and its transmission and delay due to reduced group velocity v_g inside the atomic medium. For a probe pulse of half-width $t_p \sim 150\,ns$ we observe a group delay t_d approaching $100\,ns$, corresponding to reduction of group velocity to $v_g \approx 3\,km/s$. Finally, Fig. 2E shows the resonant probe transmission as a function of the average number of photons contained in
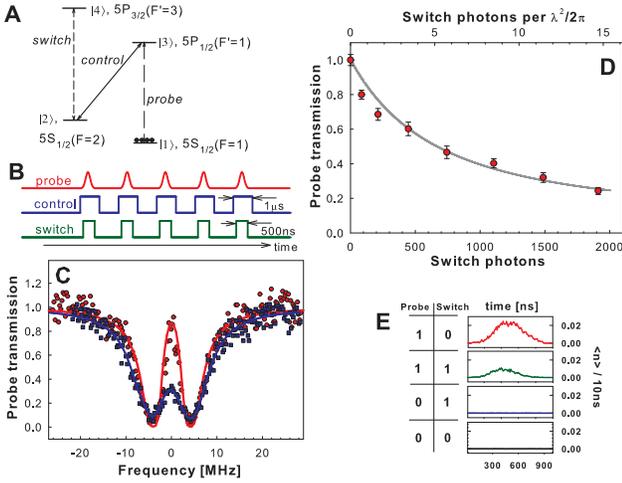
Fig. 3. (color online) (A) The atomic level scheme with corresponding hyperfine states of rubidium^{87} used in the experiment. (B) Probe, control and switch fields are broken into a set of ~ 100 synchronized pulses sent through the fiber during the off-times of the dipole trap. (C) Probe transmission through the fiber without (red) and with (blue) the switch field present. Solid lines are fits of equation (2) in Ref. [24]. (D) Observed transmission versus average number of switch photons per pulse. The solid grey line is the prediction based on equation (2) in Ref. [24]. The transmission is normalized to the EIT transmission in the absence of the switch photons. (E) Truth table of the switch, showing the detected photons in the output port of the switch system as a function of the presence of the probe and switch field pulses. Data are presented for probe pulses containing on average ~ 2 photons and with $\sim 1/e$ attenuation of transmission in the presence of the switch photons.

each control field pulse. Due to the tight confinement of light provided by the PCF, control pulses containing $\sim 10^4$ photons are sufficient to achieve almost complete transparency of an otherwise opaque system.

An efficient nonlinear optical switch can be realized by adding to the EIT Λ-system a switch field coupling the state $|2\rangle$ to an excited state $|4\rangle$ (Fig. 3A), as proposed by Harris and Yamamoto [25]. In this scheme, the switching photons interact with flipped atomic spins within the slow dark-state polariton, causing a simultaneous absorption of a probe and a switch photon [26], [27], [28].

In our experiment, an additional switching field resonant with the $F = 2 \rightarrow F' = 3$ transition of the D2 line of rubidium^{87} (Fig. 3A, B) controls the transmission through the EIT medium. As shown in Figure 3C, in the absence of the switching field (red data), we observe high transmission of the probe beam on resonance due to EIT. When the switch field is turned on, this transmission is reduced. The strength of the reduction depends on the switch field intensity, which, for a fixed switch pulse length, is determined by the number of photons contained in the switch pulse (Fig. 3D). Experimentally, we observe best switching results for switch pulses of length $t_s \approx t_p + t_d$. We find a 50% reduction of the initial transmission for a total number of ~ 700 switch photons per pulse. Figure 3E presents the truth table of our switch. In the case of no probe pulse (0/0 and 0/1 settings of the switch) only background noise from the control field is detected, which is orders of magnitude smaller than the single photon per probe pulse.

A detailed analysis of the behavior of our atomic medium

can be found in Ref. [24]. However, for the relevant case of a resonant probe field, the transmission of the probe pulse can be approximated by

$$T = \frac{\exp\left(-N_s \left(\frac{\mu_s}{\mu_p}\right)^2 \frac{3}{\pi} \frac{\lambda^2}{A} \frac{t_d}{t_p+t_d}\right)}{\sqrt{1 + \frac{16t_d^2}{\mathrm{OD}\, t_p^2}}}. \tag{4}$$

Here, N_s is the number of switch photons, we assumed that the Rabi frequency of the control field is much larger than that of the switching field, the decay rate of state $|3\rangle$ is approximately the same as of state $|4\rangle$, and we used $t_d = L/v_g \approx \frac{\mathrm{OD}\gamma_{13}}{|\Omega_c|^2}$, with L being the length of the medium. For the investigated case of a relatively weak probe transition and resulting OD ≈ 3, the delay time is small ($t_d \sim t_p$) and the probe pulse is never fully stored inside the medium. If the OD is increased (either by improving the atom loading efficiency or using a stronger probe transition), $t_d \gg t_p$ and the whole probe pulse is contained inside the medium as a dark state polariton in a mostly atomic form. In this case, it follows from equation (4) that $N_s \sim \frac{A}{\lambda^2}$ switch photons attenuate the probe pulse by a factor of $1/e$.

IV. OUTLOOKS FOR SWITCHING EFFICIENCY IMPROVEMENTS

Since the switching mechanism is based on a simultaneous absorption of a switch and a probe photon, the electric field envelopes of switch pulse and of the probe pulse have to overlap inside the atomic medium. To maintain this overlap despite the large mismatch between the propagation velocities of the two pulses, the switching pulse has to stay on during the whole time t_d the probe pulse is propagating in the medium. This in turn leads to an inefficient performance of the switch, as most of the area of the switching pulse will end up not overlapping with the probe pulse. Consequently, most of the switch photons needed to create a long switching pulse of required field intensity will go to waste. This inefficiency can be improved by matching the group velocities of the probe and switching pulses during their propagation through the atomic ensemble [29]. In this way, a full overlap between the two pulses can be maintained even when the switching pulse length is reduced to t_p, which in turn leads to a reduction of the number of switch photons needed. For t_p matched to the spectral width of the transparency window of the system, we then find that $N_s \sim \frac{A}{\lambda^2 \sqrt{OD}}$.

Alternatively, the efficiency of this switching scheme can potentially be further improved by using stationary-pulse techniques [30]. In this case, a standing wave control field from two counter-propagating beams forms an EIT Bragg grating in which the probe pulse can be completely stopped with non-vanishing photonic component. Application of this scheme inside the PCF has been proposed for single-photon-controlled switching through an interaction of single-photon stationary light pulses, with probability of interaction between two single photons scaling as $\sim OD\frac{\lambda^2}{A}$ [31].
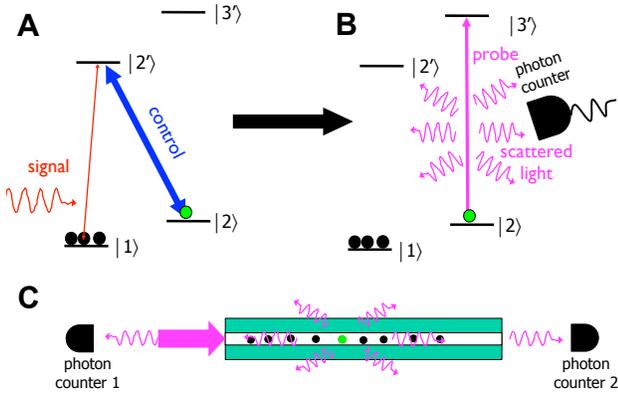
Fig. 4. (color online) Photon counting: (A) Photons are coherently stored in atomic ensemble as dark state polaritons and each photon results in a single collective excitation. (B)The ensemble is then probed with a detection laser on a cycling transition (i.e. from state $|3'\rangle$ the atom can spontaneously decay only into state $|2\rangle$), which allows scattering of multiple photons by a single excitation. (C) When the atomic ensemble is confined inside a hollow-core PCF, the scattered photons are collected and guided by the hollow fiber and detected with a photon counter. Alternatively, the presence of collective excitations can be detected by measuring the transmission of the fiber.

V. ATOM AND PHOTON DETECTION

In addition to all-optical switching, our system can be used to implement an efficient photon counting scheme proposed in Ref. [32] and [33]. This scheme combines photon storage (Fig. 4A)[34], [35] with spin-flipped atom interrogation via a cycling transition as illustrated in Fig.4B. Practical limitations in realistic atomic systems arise from experimental imperfections that can transfer the atom into state $|1\rangle$ with non-zero probability during the interrogation stage. This restricts the number of photons that can be scattered from the stored excitation, which in turn requires the scattered light to be collected with certain minimum efficiency. Implementing the photon-counting scheme with an atomic ensemble confined inside a hollow-core fiber could potentially provide the necessary efficiency boost due to collection and guiding of the scattered photons by the fiber (Fig. 4C). A necessary step on such implementation is the detection of single atoms inside the hollow-core fiber as this would indicate the capability of the system to detect and resolve single photons stored in atomic ensembles. Here we present initial experimental results of our work in this area.

When detecting small number of atoms inside the hollow fiber, the number of photons detected by the photon counter in Fig. 4 is given by

$$N_{det} = N_{sig} M_{cycl} \alpha, \qquad (5)$$

where N_{sig} is the number of atoms inside fiber, M_{cycl} is the average number of photons that can be scattered by a single atom before the atom is lost by a transfer to state $|1\rangle$ or by being heated out of the trap, and α the overall detection efficiency of the scattered photons. This relation also works for the case of photon counting with N_{sig} being the number of photons stored in the atomic ensemble. α is the product of our atom-fiber cooperativity and of the detection efficiency for photons in the guided mode of the fiber. The atom-fiber cooperativity

for an atom located at the center of the fiber (ie the probability for the atom to absorb a single photon in the mode of the fiber) is (3) 1.8% (we use linear-polarized light on the cycling $|5s_{1/2}, F = 2\rangle \rightarrow |5p_{3/2}, F = 3\rangle$ transition, because of the polarization properties of the PCF). From the optical theorem, it is equivalent to the probability for an atom inside the fiber to scatter a photon in one of the directions of the guided mode of the fiber [36]. We measure a cooperativity of 0.38% by comparing the transmission and back-scattering of resonant light out of the PCF for ensembles of ~ 100 atoms. This value is in excellent agreement with the one measured using incoherent population transfer in [18]. Although this number is compatible with a gaussian distribution with temperature 1.6mK, more detailed probing of the resonant transitions inside the dipole trap point towards the fact that a significant fraction of the atoms seem to have a radially elliptical trajectory and do not contribute highly to the atom-fiber cooperativity (Fig. 6A). This agrees with classical single-particle trajectories for atoms rolling down a bottleneck-type potential created by the dipole trap at the entrance of the fiber and starting off-center with some initial azimuthal velocity. Densities in the fiber are too low for the atomic ensemble to rethermalize. Combining the atom-fiber cooperativity with the quantum efficiency of our photon counters and coupling losses, our current setup is limited to $\alpha \sim 10^{-3}$.

The total number of photons M_{cycl} which an atom can scatter is limited by the off-resonant scattering to another state, especially inside the PCF where the clean circular polarization required for the $|5s_{1/2}, F = 2, mF = 2\rangle \rightarrow |5p_{3/2}, F = 3, mF = 3\rangle$ transition is not achievable because of birefringence and multimode effects. For the purpose of atom counting, the loss of atoms to the $|5s_{1/2}, F = 1\rangle$ state can be counteracted by periodic optical pumping. Another limiting factor to M_{cycl} is the lifetime of the atoms in the modulated dipole trap. The probing occurs during the off times of a modulated dipole trap as it is not possible to filter out dipole trap photons well enough to detect the low light level signal emanating from a few atoms. The lifetime in the modulated dipole trap is reduced to 4ms at 1MHz modulation rate due to parametric heating. Other heating mechanisms contribute to reducing the lifetime. If the atoms are probed uni-directionally in the fiber, the photon recoil accelerates the atoms, with two important consequences: the probe light is Doppler-shifted out of resonance, and the atoms rapidly escape the trap. We attribute the second effect to the mixing of the longitudinal and radial external degrees of freedom due to corrugations in the confining potential created by interference with the surface modes propagating at the core-cladding interface [37]. A clear signature of the longitudinal acceleration is the Doppler shift of the atoms and the effect can be counterbalanced by alternating probing phases with in-fiber longitudinal red-detuned molasses. Each scattering event also contributes one photon-recoil energy to the thermal energy of the atoms, due to the randomness of the emission process. The molasses can compensate the heating in the longitudinal direction. In the radial directions, the trap depth of ~ 10 mK corresponds to $\sim 10^5$ times the thermal energy gained per scattering event. In the absence of any other
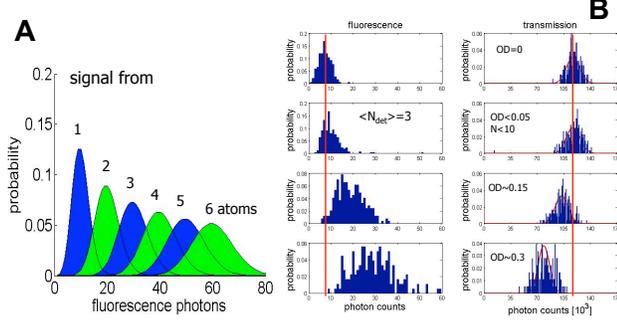
Fig. 5. (color online) (A) Effects of shot noise in detected photons on atom number resolution for $\alpha M_{cycl} = 10$. (B) Collected fluorescence and measured transmission from fiber-confined atomic ensembles of various optical depths. For the probed transition, ~ 200 atoms result in $OD \approx 1$ [18].

Fig. 6. (color online) (A.1) Probe absorption in the continuous dipole trap (blue dots). The data shows a stronger ressemblance to the expected curves for a ring-like distribution (red, A.3) than for a thermalized cloud (green, A.2). (B) In-fiber cooling can be implemented by adding a blue detuned beam to our dipole trap. The AC Stark shift along the radial axis of the dipole trap is plotted for the different Zeeman sub-levels of the $|5s_{1/2}, F = 1\rangle$ (continuous, blue), $|5s_{1/2}, F = 2\rangle$ (dashed, green) and $|5p_{1/2}, F = 2\rangle$ (dash-point, black) states in the presence of a $25\mu W$ beam, blue-detuned by 8GHz from the $|5s_{1/2}, F = 1\rangle \rightarrow |5p_{1/2}, F = 2\rangle$ transition. At the center of the trap, the blue-detuned light preferentially scatters the atoms out of $|F = 1\rangle$. When the atoms spontaneously decay back to $|F = 2\rangle$, their energy is reduced by the difference in Stark-shift between the two hyperfine ground states. A low-power repumper recycles the atoms back into $|F = 1\rangle$ away from the center of the trap, at a position where the level-shift difference is lesser. (C) Probe absorption in the dipole trap with (black,continuous) and without (red, dashed) $\sim 1ms$ of the cooling scheme described above. In the presence of cooling, the narrowed absorption profile results from the atoms being radially cooled to the bottom of the trap, although we simultaneously observe atoms loss out of the trap.

heating mechanism and using a resonant probe at saturation intensity, M_{cycl} is restricted by the lifetime of the atoms in the modulated dipole trap to $\sim 10^4$.

The atom number (and eventually photon number) resolution in this system is limited by the shot noise of detected photons, and we get from equation (5) that the uncertainty in measured photon number would be

$$\Delta N_{sig} = \frac{N_{det}^{\frac{1}{2}}}{\alpha M_{cycl}} = \left(\frac{N_{sig}}{\alpha M_{cycl}}\right)^{\frac{1}{2}} \quad (6)$$

Figure 5A plots the probabilities of detecting a particular number of photons for various number of atoms present in the fiber. For the parameters of our system, we see that the resolution of atom number becomes more difficult as the atom number increases over just a few.

Fig. 5B shows our initial experimental results. Here, we observed the fluorescence (photon counter 1 in Fig. 4C) and transmission (photon counter 2 in Fig. 4C) of atoms loaded into the fiber and probed on the cycling transition. The data is compared with the signal obtained from an empty fiber. We were able to detect as few as ~ 10 atoms using the scattered light, when the atoms could not be observed in the transmission signal anymore. However, atoms disappear from the dipole trap after scattering only ~ 350 photons/atom. This value is independent of density, which excludes light assisted collisions as possible cause. It is also independent of trap depth, which excludes the simple heating mechanisms described above. We attribute this effect to the non-perfect linear polarization of the dipole trap, especially in the presence of surface modes. For a perfectly circular polarization, the dipole trap acts as a fictitious magnetic field and two successive Zeeman sub-levels are shifted (for $|5s_{1/2}, F = 1\rangle$) by $\sim 40MHz$ for our parameters. At each turn-on of the dipole trap, the probe has reshuffled the population between the Zeeman sublevels. These energy fluctuations increase the thermal energy of the atoms by the Zeeman splitting at each cycle of the dipole trap. A few percent of circularly polarized light is enough to account for the atoms escaping the trap in the absence of radial cooling (the heating in the longitudinal direction is reduced by the optical molasses). Fig. 6B describes a way to cool the atoms without radial access by adding a weak blue-
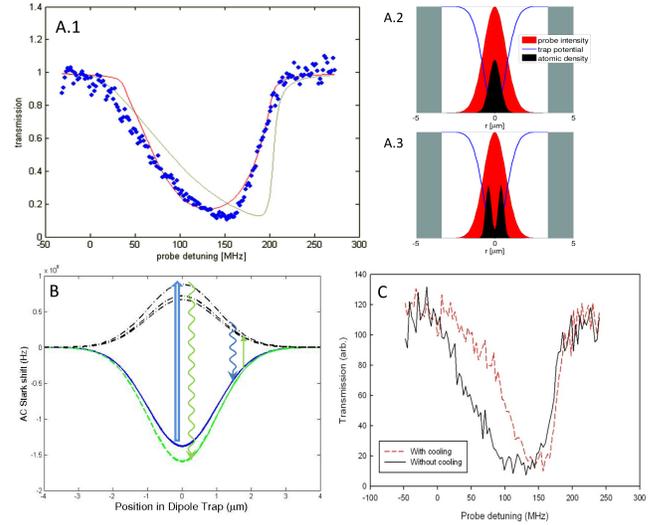
detuned (a few GHz to the $|5s_{1/2}, F = 2\rangle \rightarrow |5p_{1/2}, F = 1\rangle$ transition) and a weak repumper beam close to the free space resonance. For each depicted cycle, the atoms cool by an energy corresponding to the peak energy difference between the Stark-shifted hyperfine states. Fig. 6C displays preliminary results of this cooling method inside the PCF. After a few ms of cooling, the absorption in the dipole trap indicates that the atoms have radially cooled to the bottom of the trap. Some losses occur during the process and we are currently working on improving this effect.

While the system in its current form is not suitable for photon number detection, its weak spots can be fixed in the future. In particular, improvement of the atom-fiber cooperativity by an order of magnitude would allow robust photon number resolution. This could be achieved by in part by additional cooling and increased confinement of the atoms inside the fiber, but most directly by using a hollow waveguide with smaller diameter of the guided mode, such as the one demonstrated in Ref. [38].

VI. CONCLUSION

With the fiber acting as a guide for both photons and atoms, the photons can interact with an optically dense atomic ensemble without being limited by diffraction. This makes the

system an excellent candidate for nonlinear optics at very low light levels [24], while the large optical depth achievable in this system [18] makes it ideally suited for the implementation of schemes for enhancing optical nonlinearities and creating effective photon-photon interactions [31], [39], [40], [41], [42], [43]. Finally, while the experiments discussed here were performed in a vacuum chamber containing a piece of hollow-core PCF, recent developments in design and fabrication of integrated hollow optical waveguides [44], [45] open the possibilities for developing this system into a scalable on-chip architecture.

REFERENCES

[1] K. M. Birnbaum, A. Boca, R. Miller, A. D. Boozer, T. E. Northup, and H. J. Kimble, "Photon blockade in an optical cavity with one trapped atom," *Nature*, vol. 436, p. 87, 2005.

[2] T. Wilk, S. C. Webster, A. Kuhn, and G. Rempe, "Single-atom single-photon quantum interface," *Science*, vol. 317, pp. 488 – 490, 2007.

[3] I. Fushman, D. Englund, A. Faraon, N. Stoltz, P. Petroff, and J. Vuckovic, "Controlled phase shifts with a single quantum dot," *Science*, vol. 320, no. 5877, pp. 769–772, 2008.

[4] B. Dayan, A. S. Parkins, T. Aok, E. Ostby, K. Vahala, and H. Kimble, "A photon turnstile dynamically regulated by one atom," *Science*, vol. 319, no. 5866, pp. 1062–1065, 2008.

[5] J. Beugnon, C. Tuchendler, H. Marion, A. Gaëtan, Y. Miroshnychenko, Y. R. P. Sortais, A. M. Lance, M. P. A. Jones, G. Messin, A. Browaeys, and P. Grangier, "Two-dimensional transport and transfer of a single atomic qubit in optical tweezers," *Nature Physics*, vol. 3, p. 696, 2007.

[6] R. Cregan, B. Mangan, J. Knight, T. Birks, P. Russell, P. Roberts, and D. Allan, "Single-mode photonic band gap guidance of light in air," *Science*, vol. 285, pp. 5433, pp. 1537 – 1539, 1999.

[7] D. Yin, H. Schmidt, J. P. Barber, and A. R. Hawkins, "Integrated arrow waveguides with hollow cores," *Optics Express*, vol. 12, p. 2710, 2004.

[8] L. M. Tong, R. R. Gattass, J. B. Ashcom, S. L. He, J. Y. Lou, M. Y. Shen, I. Maxwell, and E. Mazur, "Subwavelength-diameter silica wires for low-loss optical wave guiding," *Nature*, vol. 426, p. 816, 2003.

[9] R. M. Dickson and L. A. Lyon, "Unidirectional plasmon propagation in metallic nanowires," *J. Phys. Chem. B*, vol. 104, p. 6095, 2000.

[10] J. D. Joannopoulos, R. D. Meade, and J. N. Winn, *Photonic Crystals: Molding the Flow of Light*. Princeton University Press, 1995.

[11] B. E. A. Saleh and M. C. Teich, *Fundamentals of Photonics*, 2nd ed. Wiley-Interscience, 1997.

[12] F. Benabid, F. Couny, J. C. Knight, T. A. Birks, and P. S. Russell, "Compact, stable and efficient all-fibre gas cells using hollow-core photonic crystal fibres," *Nature*, vol. 434, p. 488, 2005.

[13] F. Benabid, J. Knight, G. Antonopoulos, and P. Russell, "Stimulated raman scattering in hydrogen-filled hollow-core photonic crystal fiber," *Science*, vol. 298, no. 5592, pp. 399–402, OCT 11 2002.

[14] S. O. Konorov, A. B. Fedotov, and A. M. Zheltikov, "Enhanced four-wave mixing in a hollow-core photonic-crystal fiber," *Opt. Lett.*, vol. 28, pp. 1448 – 1450, 2003.

[15] S. Ghosh, A. R. Bhagwat, C. K. Renshaw, S. Goh, A. L. Gaeta, and B. J. Kirby, "Low-light-level optical interactions with rubidium vapor in a photonic band-gap fiber," *Phys. Rev. Lett.*, vol. 97, no. 2, p. 023603, 2006.

[16] T. Takekoshi and R. J. Knize, "Optical guiding of atoms through a hollow-core photonic band-gap fiber," *Phys. Rev. Lett.*, vol. 98, no. 21, p. 210404, 2007.

[17] C. A. Christensen, S. Will, M. Saba, G.-B. Jo, Y.-I. Shin, W. Ketterle, and D. Pritchard, "Trapping of ultracold atoms in a hollow-core photonic crystal fiber," *Phys. Rev. A*, vol. 78, no. 3, p. 033429, 2008.

[18] M. Bajcsy, S. Hofferberth, T. Peyronel, V. Balic, Q. Liang, A. S. Zibrov, V. Vuletic, and M. D. Lukin, "Laser-cooled atoms inside a hollow-core photonic-crystal fiber," *Phys. Rev. A*, vol. 83, p. 063830, 2011.

[19] R. Grimm, M. Weidemuller, and Y. Ovchinnikov, "Optical dipole traps for neutral atoms," *Adv. in Atomic, Molec., and Opt. Physics*, vol. 42, pp. 95–170, 2000.

[20] S. Harris, "Electromagnetically induced transparency," *Phys. Today*, vol. 50, pp. 36 – 42, 1997.

[21] M. Fleischhauer, A. Imamoğlu, and J. Marangos, "Electromagnetically induced transparency: Optics in coherent media," *Rev. Mod. Phys.*, vol. 77, p. 633, 2005.

[22] M. Fleischhauer and M. D. Lukin, "Dark-state polaritons in electromagnetically induced transparency," *Phys. Rev. Lett.*, vol. 84, pp. 5094 – 5097, 2000.

[23] L. Hau, S. Harris, Z. Dutton, and C. Behroozi, "Light speed reduction to 17 metres per second in an ultracold atomic gas," *Nature*, vol. 397, no. 6720, pp. 594–598, 1999.

[24] M. Bajcsy, S. Hofferberth, V. Balic, T. Peyronel, M. Hafezi, A. S. Zibrov, V. Vuletic, and M. D. Lukin, "Efficient all-optical switching using slow light within a hollow fiber," *Phys. Rev. Lett.*, vol. 102, p. 203902, 2009.

[25] S. Harris and Y. Yamamoto, "Photon switching by quantum interference," *Phys. Rev. Lett.*, vol. 81, p. 3611, 1998.

[26] M. Yan, E. Rickey, and Y. Zhu, "Observation of absorptive photon switching by quantum interference," *Phys. Rev. A*, vol. 64, p. 041801(R), 2001.

[27] D. Braje, V. Balic, G. Yin, and S. Harris, "Low-light-level nonlinear optics with slow light," *Phys. Rev. A*, vol. 68, p. 041801(R), 2003.

[28] Y. Chen, Z. Tsai, Y. Liu, and I. Yu, "Low-light-level photon switching by quantum interference," *Opt. Lett.*, vol. 30, p. 3207, 2005.

[29] M. Lukin and A. Imamoğlu, "Nonlinear optics and quantum entanglement of ultraslow single photons," *Phys. Rev. Lett.*, vol. 84, p. 1419, 2000.

[30] M. Bajcsy, A. S. Zibrov, and M. D. Lukin, "Stationary pulses of light in an atomic medium," *Nature*, vol. 426, pp. 638–641, 2003.

[31] A. André, M. Bajcsy, A. S. Zibrov, and M. D. Lukin, "Nonlinear optics with stationary pulses of light," *Phys. Rev. Lett.*, vol. 94, no. 6, p. 063902, 2005.

[32] A. Imamoğlu, "High efficiency photon counting using stored light," *Phys. Rev. Lett.*, vol. 89, no. 16, p. 163602, OCT 14 2002.

[33] D. James and P. Kwiat, "Atomic-vapor-based high efficiency optical detectors with photon number resolution," *Phys. Rev. Lett.*, vol. 89, p. 183601, 2002.

[34] D. F. Phillips, A. Fleischhauer, A. Mair, R. L. Walsworth, and M. D. Lukin, "Storage of light in atomic vapor," *Phys. Rev. Lett.*, vol. 86, pp. 783–786, 2001.

[35] C. Liu, Z. Dutton, C. H. Behroozi, and L. Hau, "Observation of coherent optical information storage in an atomic medium using halted light pulses," *Nature*, vol. 409, pp. 490 – 493, 2001.

[36] H. Tanji-Suzuki, I. Leroux, M. Schleier-Smith, M. Cetina, A. Grier, J. Simon, and V. Vuletic, "Interaction between atomic ensembles and optical resonators: Classical description," *Adv. At. Mol. Opt. Phys.*, vol. 60, pp. 201–237, 2011.

[37] J. West, C. Smith, N. Borrelli, D. Allan, and K. Koch, "Surface modes in air-core photonic band-gap fibers," *Opt. Express*, vol. 12, pp. 1485–1496, 2012.

[38] G. S. Wiederhecker, C. M. B. Cordeiro, F. Couny, F. Benabid, S. A. Maier, J. C. Knight, C. H. B. Cruz, and H. L. Fragnito, "Field enhancement within an optical fibre with a subwavelength air core," *Nature Photonics*, vol. 1, p. 115, 2007.

[39] M. Fleischhauer, J. Otterbach, and R. G. Unanyan, "Bose-einstein condensation of stationary-light polaritons," *Phys. Rev. Lett.*, vol. 101, p. 163601, 2008.

[40] D. Chang, V. Gritsev, G. Morigi, V. Vuletic, M. Lukin, and E. Demler, "Crystallization of strongly interacting photons in a nonlinear optical fiber," *Nature Physics*, vol. 4, pp. 884 – 889, 2008.

[41] J. Otterbach, R. G. Unanyan, and M. Fleischhauer, "Confining stationary light: Dirac dynamics and klein tunneling," *Phys. Rev. Lett.*, vol. 102, p. 063602, 2009. [Online]. Available: http://link.aps.org/doi/10.1103/PhysRevLett.102.063602

[42] J. Otterbach, J. Ruseckas, R. G. Unanyan, G. Juzeliūnas, and M. Fleischhauer, "Effective magnetic fields for stationary light," *Phys. Rev. Lett.*, vol. 104, p. 033903, 2010.

[43] A. V. Gorshkov, J. Otterbach, E. Demler, M. Fleischhauer, and M. D. Lukin, "Photonic phase gate via an exchange of fermionic spin waves in a spin chain," *Phys. Rev. Lett.*, vol. 105, p. 060502, 2010.

[44] W. Yang, D. B. Conkey, B. Wu, D. Yin, A. R. Hawkins, and H. Schmidt, "Atomic spectroscopy on a chip," *Nature Photonics*, vol. 1, p. 331, 2007.

[45] Q. M. Quan, I. Bulu, and M. Loncar, "Broadband waveguide qed system on a chip," *Phys. Rev. A*, vol. 80, p. 011810, 2009.

Michal Bajcsy is currently postdoctoral scholar in Ginzton Laboratory at Stanford University. He received his PhD in Applied Physics from Harvard University in 2010.

Sebastian Hofferberth received his PhD in Physics from Universität Heidelberg in 2007. He spent his postdoctoral years at Harvard and MIT at the Center for Ultracold Atoms and is now at Universität Stuttgart.

Thibault Peyronel is a graduate student in the Physics Department at Massachusetts Institute of Technology.

Vlatko Balic received his PhD in Physics from Stanford University. He spent two years as a postdoctoral researcher at Harvard University and CUA.

Mohammad Hafezi is currently a research associate at JQI at University of Maryland. He received his PhD in Physics from Harvard University in 2010.

Qiyu Liang is a graduate student in the Physics Department at Massachusetts Institute of Technology.

Alexander S. Zibrov is currently a researcher at MIT-Harvard Center for Ultracold Atoms. He has previously worked at the Harvard-Smithsonian Center for Astrophysics, NIST, and Lebedev Physical Institute.

Vladan Vuletic is a Professor of Physics at at Massachusetts Institute of Technology. He received his PhD from Ludwig-Maximilians-Universität München.

Mikhail D. Lukin is a Professor of Physics at Harvard University. He received his PhD from Texas A&M University.